Robust MIMO Control of a Parallel Kinematics Nano-Positioner for High Resolution High Bandwidth Tracking and Repetitive Tasks

Jingyan Dong, Srinivasa M. Salapaka, Placid M. Ferreira

Abstract—This paper presents the design and implementation of robust control schemes for two applications of a nanopositioning stage (1) reference trajectory tracking with high resolution over a given bandwidth (2) control design for repetitive motions. The stage has a low degree of freedom monolithic parallel kinematic mechanism using flexure hinges. It is driven by piezoelectric actuators and its displacement is detected by capacitance gauges. The design has strongly coupled dynamics with each actuator input producing in multiaxis motions. The nano-positioner is modeled as a multiple input and multiple output (MIMO) system, and the MIMO plant model is identified by time-domain identification methods. The design of the nano-positioner relies heavily on the control design to account for the high coupling in the system. The proposed H₁₀ MIMO controller achieves a good performance in terms of resolution, bandwidth and robustness to the modeling uncertainty. In the second part of the paper, we present control design for tasks that require repetitive motion of nano positioning system. These tasks are quite common in micro/nano manipulation and manufacturing. This paper presents a robust control design that gives a significant (over thirty fold) improvement in tracking of repetitive motions on a prespecified frequency band. This design, unlike other schemes, is robust to modeling uncertainties that arise in flexure based mechanisms, and does not require any learning steps during its real time implementation. This design scheme is implemented on a parallel-kinematics XYZ nano positioning stage for repetitive nano-manipulation and nano-manufacturing applications.

I. INTRODUCTION

Multi-axis micro and nanopositioning systems are increasingly used in most of the modern micro and nano technology. Typically, nano-positioner designs focus on single degree of freedom axis modules and realize multi-axes systems by stacking individual units together. From a kinematics point of view, these designs belong to the class of serial kinematics systems in which the axes of motion are connected serially from a fixed base to the end effector to

Jingyan Dong is with Department of Mechanical Science and Engineering, University of Illinois at Urbana-Champaign, (e-mail: jdong@uiuc.edu).

Srinivasa M. Salapaka, is with Department of Mechanical Science and Engineering, University of Illinois at Urbana-Champaign, (phone: 217 244-4172; fax: 217 244-6534; e-mail: salapaka@uiuc.edu)

Placid M. Ferreira is with Department of Mechanical Science and Engineering, University of Illinois at Urbana-Champaign, (e-mail: pferreir@uiuc.edu).

This material is based upon work supported by the National Science Foundation through the Center for Nanoscale Chemical Electrical and Mechanical Manufacturing Systems under Award Number DMI 0328162, through Award Number Grant DMI 0422687, and through Award Number ECS 0449310 CAR.

form an open kinematic chain. These designs [1-6] are easy to implement and build from, but they tend to have relatively large inertias and relatively low dynamic stiffness of the resulting systems. In addition, these designs use different masses for motion in each axis that result in different natural frequencies and performance capabilities along different axes, which in some instances are undesirable. Parallel kinematic mechanisms (PKM) overcome the above problems by having multiple kinematic chains that connect the base and end effector in a parallel scheme. Parallel kinematics designs usually have high structural stiffness due to their and truss-like structure shorter kinematic Applications of different parallel kinematics designs for micro/nanopositioning stages have also been reported [7-13].

Control design for serial kinematics systems is relatively simple because each actuation maps to a single direction of motion, orthogonal to the others and are thus decoupled. The dynamics along each axis can easily be described by SISO system. Recently these SISO control designs have yielded significant improvement in performance in terms of repeatability and bandwidth for a given resolution [14-17]. For the parallel kinematics systems, control design can be pretty complex as such decoupling is often not possible as the influence vectors of the actuators may not be orthogonal. For this parallel kinematics mechanism, depending on the feedback methods, there are two control configurations. The first control configuration is to control the motion of each individual joint [8,16]. Forward kinematics and inverse kinematics describe the relationship between joint positions and XYZ displacement. This direct joint control makes control design relatively easy and a simple SISO design is sufficient. However, this control scheme is susceptible to manufacturing inaccuracies and, flexural deflections of the links and clearances and friction in the unactuated joints.

The other control configuration is to control directly the position in XYZ space. In this case, the feedback variables are displacements in XYZ direction. In this configuration, all three joints are coupled together and as a consequence, actuation of one joint may produce an output motion with components along multiple axes in the task space. Thus, this positioning stage is a coupled multiple input and multiple output (MIMO) system, which makes the control design and implementation relatively difficult. In this paper, modern robust control theory is applied to a parallel kinematic XYZ nano positioner to simultaneously achieve high bandwidth, resolution and robustness. Besides the plant being a strongly

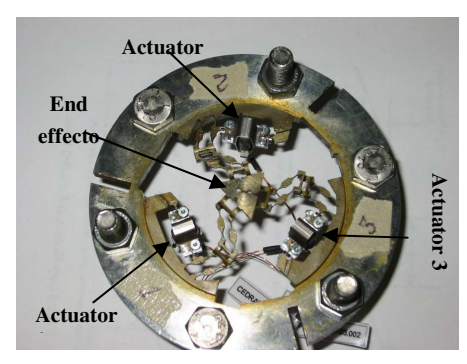


Figure 1: The PKXYZNP prototype

coupled MIMO system, the complexity in the control design is further aggravated by the proximity of the plant's poles to the imaginary axis as a consequence of the low damping provided by the flexure based structures. In this paper, the design and characteristic of the PKM nano positioning device is introduced and then its dynamic model is identified. An H_{∞} controller is synthesized to achieve required performance.

In the later part of the paper, the issue of achieving high resolution but fast repetitive motions from the nanopositioner is presented. These repetitive tasks are quite common in Micro/nano manipulation and manufacturing. In these devices there is an inherent trade-off between the bandwidth and the resolution. The control scheme identifies this trade-off and appropriately designs a controller that achieves fast motions while at the same time keeping a very high resolution.

II. DEVICE DESCRIPTION

The parallel-kinematics XYZ nanopositioning stage and a schematic of its kinematics model are shown in Fig. 1. The detailed design, kinematics analysis and dynamics analysis are described in [12,13]. In this design, three independent kinematic chains connect the base and the end effector (the triangular table at the centre in parallel. Each kinematic chain is comprised of two parallelogram four-bar mechanisms, which makes the connector always parallel to the base. Together the three kinematic chains restrict all rotational degrees-of-freedom at the table, leaving it with three translations to satisfy the constraints imposed by the three kinematic chains.

The actual mechanical component of the stage is fabricated as a monolithic structure using electro-discharge machining (EDM). A set of piezoelectric actuators were chosen to actuate each of these kinematics chains at the first four-bar mechanism, that is connected to the base. The overall size of the stage is about 5cm in length and width and 2cm in height. The position sensing system consists of three capacitance sensors and a target that has three orthogonal. For this setup, calibration is relatively easy and the resolution obtained is significantly higher than sensing the displacement from each joint. As we stated before, sensing and controlling joints

motion will bring three SISO control system, however the task positions totally depend on kinematics interpolation, which is vulnerable to manufacturing and calibration error. The stage design parameters along with an allowable hinge rotation produced a maximum displacement of about 87 μm along each axis and a work zone of $3.223 \times 10^4 \mu m^3$. The detailed workspace analysis is presented in [12, 13].

The static relationship between the displacement of each joint and the motion in the task space can be described by the forward kinematics and inverse kinematics. In [12,13], by analyzing the geometry of the system, the kinematics problem is solved. The XYZ motion are functions of joint angles α, β, γ , $X = X(\alpha, \beta, \gamma), Y = Y(\alpha, \beta, \gamma), Z = Z(\alpha, \beta, \gamma)$. The velocity of the end-effector is related to the angular velocities of the joints by Jacobian matrix, p = Jq.

In the stage, the displacement of the end-effector as well as joints are very small, compared with the dimension of the overall mechanism. Linearization of the kinematics at the operating point gives following relationship between joint and end-effector position $[\Delta x, \Delta y, \Delta z] = J[\Delta \alpha, \Delta \beta, \Delta \gamma]$.

III. MODEL IDENTIFICATION

The analysis of the positioning system and its control design requires an accurate dynamical model. The PKM nano positioning stage has a very complex mechanical structure and it is extremely difficult to physically model the dynamic behavior of such a system accurately. In this paper, a linear model of the system is identified experimentally about an operating point and the uncertainty in the model is accounted for by designing the control algorithm for robustness in addition to other performance criteria such as bandwidth and resolution. At an operating point at 0 V for all the actuators, we represent this system by a 3-by-3 transferfunction matrix. $P_{X,Y,Z}(s) = G_{3x3}(s)V_{A,B,C}(s)$. Here $V_{A,B,C}(s)$ is a vector of voltage inputs of three piezoelectric actuators and $P_{X,Y,Z}(s)$ is a vector position in X, Y and Z directions. Since the PKM design distributes the load and the motion to different axes, it is impossible to decouple the inputs for the actuator and the displacement outputs from the stage.

Time domain identification tools from the systems theory [18] instead of the frequency domain based method were used to obtain the dynamical model of the system so as to avoid large amplitude vibrations at the resonant frequencies which can damage flexure structures by plastic deformation. A modified pseudo random binary signal is used as the input signal. These signals, where their energy is distributed over the whole range of the spectrum are gentle on lightly-damped resonances. A signal is sent to each input channel of the stage and the corresponding three outputs are recorded and analyzed. By using parametric model estimation approach, a 3-by-1 transfer function matrix is identified for each input channel, which corresponds to one column of the overall

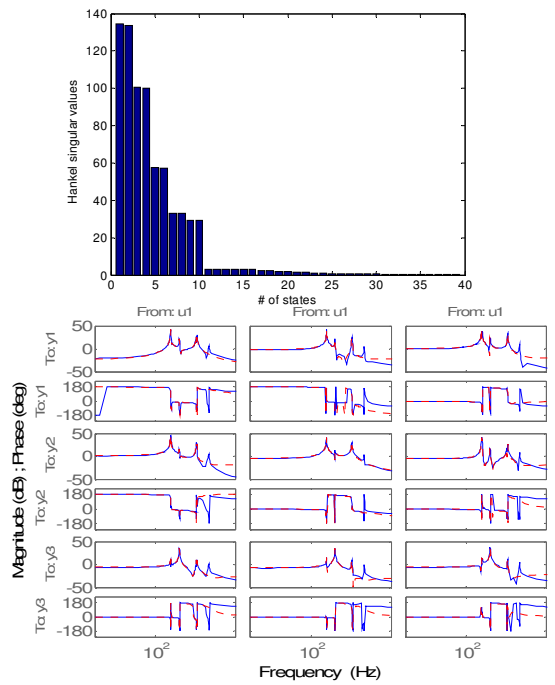


Figure 2. Hankel singular values of the model and comparison of frequency response between model (solid) and reduced rank model (dashed)

transfer function matrix.

An input signal was generated by combining pseudo random binary signals with a step input signal, which was used to identify the DC gain and low frequency response accurately. The response of identified model fits to the experimental response extremely well. The fit factors [19] for all nine transfer functions are all larger than 88%.

The frequency response of identified model is shown in Fig. 2(b). From the bode plots, we observe that there are 6 main modes for the system, at frequencies near 175 Hz, 179 Hz, 245 Hz, 460 Hz, 474 Hz, 740 Hz. Among these modal frequencies, 175 Hz, 179 Hz, 460 Hz, 474 Hz are related to the response in the X and Y directions and 245 Hz & 740 Hz correspond to the motion along the Z axis. From the design of the device, the three kinematics chains are designed symmetrically in XY plane. Therefore, it can be expected that, for an ideal system, any direction in XY plane can be modal directions and share the same modal frequency. However, imperfections in fabrication will result in specific modal direction, and very close frequencies. The model further validates the low damping in our flexure based design where the damping factor is less than 0.01 for all the modes.

The mechanical structure of our positioning stage results in almost linear motion. However, the piezoelectric actuator has nonlinearity such as hysteresis. The model identified at different operating points demonstrates this effect. We find that the differences at low frequencies (<5 Hz) are much larger than at high frequencies. These differences are easily taken care of by designing high gain controllers (specially at low frequencies), nevertheless, this model uncertainty adds to the need for robustness in control design.

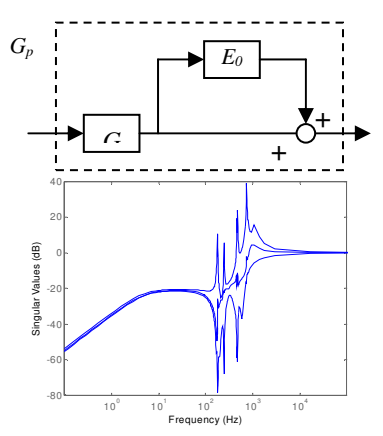


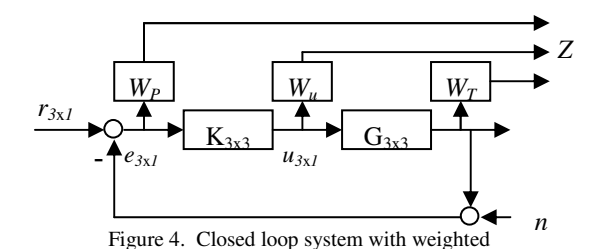
Figure 3. Multiplicative output uncertainty (a) and Singular value for uncertainty $E_0\left(b\right)$ from model reduction

IV. Nominal H_{∞} Control Design For High Bandwidth

The primary objective of control design is to achieve a stage with high precision positioning and high bandwidth tracking capability that is robust to uncertainties in the operating conditions. These objectives are to be met under the limitations on the control signal of the piezoelectric actuator. High precision requirements in target applications such as tool placement place stringent demands for high resolution. This makes it necessary that the closed loop system rejects the disturbances and attenuates noise over the bandwidth of interest. High throughput requirements of the target applications make high bandwidth a necessity. The requirement for reliably good positioning capability under changing operating conditions makes it important to account for robustness in the control design.

We fit a 39th order model for the positioning system (a 13th order transfer function for each column in $G_{3\times3}(s)$) in the previous section. We obtained a reduced order model for the positioning system by obtaining truncating the balanced realization of its identified model. Fig.2(a) shows the Hankel singular values of the balanced realization of the model. The first ten states dominate the input/output characteristic. Thus the last 29 states are removed while keeping the DC gain of the reduced order model equal to the original model. The bode plot of reduced order model matches well with the original model (see Fig.2 (b)).

The approximation error in using the reduced order model as the nominal model for the positioning system is viewed as output modeling uncertainty given by $G_P(s) = (I + E_o)G$. Here $G_P(s)$ represents the actual system, which is viewed as a perturbation of the nominal reduced order model G(s), $E_o = (G_P - G)G^{-1}$ represents the model uncertainty. The singular value of E_o is shown in Fig. 3. Note that the model reduction error is relatively low at low frequency (< -20 dB below 140 Hz), and high at high frequency (large than 0 dB



when frequency above 600 Hz). However, between 140Hz and 600Hz, there are three peaks corresponding to the modes of the system at about 175 Hz, 245 Hz, and 465 Hz. These peaks indicate large model uncertainty at the structural modes that places a greater emphasis on the need for robust control design.

 H_{∞} robust control approach is applied to design the control law for our parallel kinematic nano-positioning system. The closed loop diagram with weighted outputs is shown in Fig.4. We designed the weighting functions to shape the sensitivity function S, the complimentary sensitivity transfer function T and control transfer function KS. W_P is the weight on S, which describes the performance objectives of good tracking bandwidth. W_T is the weight on T, which shapes the performance objectives of noise rejection and W_u is the weight on KS so as to bound control signal to be under saturation limits. In the control design, the controller is chosen so as to satisfy the following criterion: $\|W_p S, W_T T, W_u KS\|_{\max} \le 1$. The transfer function W_P is chosen to have high gain at low frequency and low gain at high frequency. For our system, the W_P is chosen as $W_p(s) = \frac{0.6667 \text{ s} + 314.2}{\text{s} + 0.03142}$, which is designed to make

sensitivity function has an input-to-error gain 0.01% at low frequency and a bandwidth of 50 Hz. The high frequency noise attenuation is imposed by designing the weight W_T on T. W_T is chosen to have high gains at high frequencies so as to make complimentary sensitivity transfer function T small at high frequencies. Thus T rolls off at high frequencies. We

designed
$$W_T(s) = \left(\frac{s + 314.2}{0.001 \text{ s} + 628.3}\right)^2$$
, with a high frequency

gain of 120 dB and a rolling off rate of 40 dB slope. We need this high rolling off rate to decrease the effect of uncertainty peak at 175 Hz. The weighting function for control signal is chosen to be a constant as W_u =0.15 so as that the control signal for actuator will not over its requirement limits.

 $\|W_pS,W_TT,W_uKS\|_{\max} \le \gamma$. For the weighting transfer functions we used above, we get a nineteenth order controller with $\gamma = 1.34$. Fig. 5 shows the singular value plots of the sensitivity transfer functions with the full order model. Due to the model reduction error, the controller designed from reduced order model brings several peaks for sensitivity function, however, the maximum peak $\|S\|_{\max}$ is less than 1.85

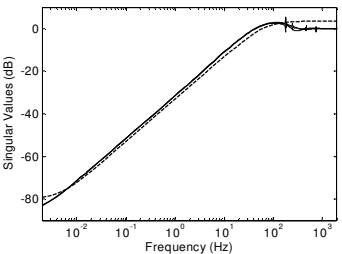


Figure 5. Sensitivity function for full rank model. Target sensitivity function (dashed). Achieved functions (solid).

(5.25 dB). The small peak indicates good robustness to the

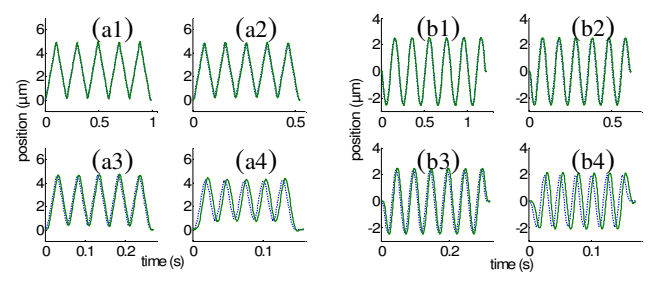


Figure 6. Tracking of triangular (a) and sinusoidal (b) waves at (a1, b1) 5Hz, (a2, b2) 10Hz, (a3, b3) 20Hz, (a4, b4) 40Hz. Reference: dotted. Output: solid

uncertainties inside the system. The singular value plots of the sensitivity transfer function and the closed loop transfer function gives the corresponding crossover frequencies are 32 Hz and 59 Hz.

To demonstrate the tracking performance of the stage, triangular and sinusoidal waves at different frequencies are sent to the stage and output is plotted in Fig. 6. The closed loop system tracks these signals pretty well for 5Hz to 20 Hz signals. For 40 Hz triangular signal, the command signals as well as outputs get round off at the corner, due to the interpolation capabilities of the controller. Besides that, the control system even tracks 40 Hz well except for phase shift.

V. CHARACTERIZATION OF THE CLOSED-LOOP DEVICE

Hysteresis is a common nonlinearity for piezoelectric actuators. The displacement of piezoelectric actuators cannot follow a linear relationship with actuation voltage, which significantly limits the positioning resolution. For our PKXYZNP stage, the displacement of a single actuator will affect the motion in all XYZ directions. Thus the hysteresis effect is attributed to all the directions. Fig. 7 demonstrates an example of hysteresis curve in our system. Actuation voltage is applied to an actuator gradually from 0 volt to 1.65 volts, which corresponds to the motion about -10 µm, 7.1µm and 5.4µm, in XYZ directions. It can be easily found out that the maximum output hysteresis is about 1.5 µm (15%), the maximum input hysteresis is about 0.23V (14%). However H_{∞} robust control effectively compensates this nonlinear effect. In Fig.7 (B), a reference command is given to an axis moving that axis from origin to 20 µm and then moving back. Virtually H_{\infty} robust control design removes all the hysteresis effect. The maximum output and input

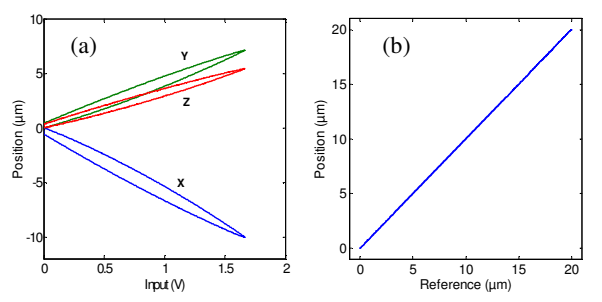


Figure 7. Hysteresis in open loop (a) and closed loop configuration (b)

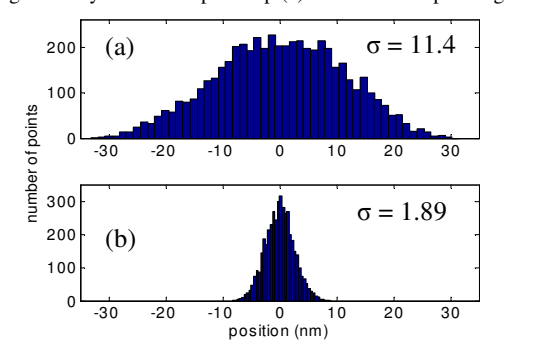


Figure 8. sensor measurements of steady state positions (a) open loop (b) closed loop

hysteresis is about 20 nm, only 0.1% of overall input and output range. These hysteresis experiments also validate using the linear model that we identified only about one operating point. However as clearly seen from these experimental results, the closed loop system gives desired (linear) motion for the entire range for motion of the system and it is insensitive to the error from simplification that we assumed in the open loop model.

Resolution is an important performance for positioning system. In our flexure based system, reference signals in XYZ directions are directly controlled, the resolution is primarily restricted by noise. Due to the low damping of the mechanical structure, this high frequency noise will vibrate the stage and deteriorate the positioning resolution. By designing roll-off frequency and roll-off rate of T, the noise can be suppressed greatly. This determines the trade off between the resolution and the bandwidth of the system. Figure 8 demonstrates the steady-state output from a sensor under open loop as well as closed loop configuration. The standard deviation of the output signal is 11.4 nm for open loop configuration, while the value for closed loop reading is only 1.89 nm. These results clearly demonstrate the great improvement of the resolution under H_{∞} robust control. Reducing the bandwidth will result in a better resolution.

VI. H_{∞} Control Design For Repetitive Nano-Positioning Tasks

Normally, H_{∞} control design has the low pass type of sensitivity transfer function which provides a good tracking performance only at relatively low frequencies. But at the frequency close to the bandwidth of the system, the tracking performance is degraded. In micro/nano manipulation, tasks

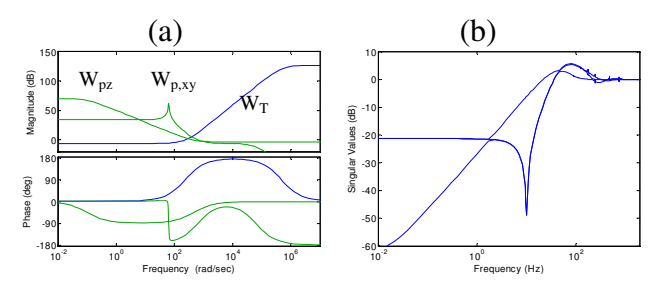


Figure 9. Weight functions (a) and closed loop sensitivity function (b)

that require repetitive motion of nano positioning systems are quite common. Consequently, typical designs do not achieve high tracking performance for fast repetitive motions. Typical approaches that are designed to improve the tracking performance for repetitive motion are repetitive control. These control strategies incorporate the information from previous cycles to improve the tracking performance. Thus learning cycles are necessary for such controllers, which prevent them from real time implementation.

In the section, robust control approach is applied to design a controller that focus on the performance over a specific frequency band. Instead of designing a low pass type of sensitivity function, a band pass sensitivity transfer function is used. For our device, repetitive motions are mostly in XY plane and Z motion is only for holding the sample. Thus different sensitivity weighting transfer functions are chosen for XY and Z motion. It should also be remarked that the frequency range of the command signals are known a priori and thus this design scheme achieves a good tracking performance in this range at the cost of losing performance at other frequency ranges. This design is very well suited for tasks such as scanning where high resolution fast motions are more important than the specific time signals employed for scanning. For our system, the W_P for X and Y transfer

function is $W_{p,xy}(s) = \frac{0.5 \text{ s}^2 + 628.3\text{s} + 1.974\text{e}5}{2.53\text{e} - 10 \text{ s}^4 + 3.18\text{e} - 5\text{s}^3 + \text{s}^2 + 2.64\text{s} + 3948}$, so as

to achieve best performance at 10 Hz. For Z motion, since it is not involved in the periodical movement, its sensitivity weighting transfer function keeps same. We also keep W_T unchanged so as to provide the high rolling off rate to decrease the effect of uncertainty. Figure 9 (a) shows an example of weighting transfer functions.

 $\|W_pS,W_TT,W_pKS\|_{\max} \leq \gamma$. For weighting transfer functions we used above, we get a 25^{th} order controller with $\gamma=4.3$. The singular value plots of the sensitivity transfer functions are shown in Fig. 9(b). For X and Y, sensitivity transfer functions have a lowest peak at 10 Hz about -50 db, which brings an error-to-input gain 0.003 at that frequency. Since the sensitivity weighing functions are carefully designed, although a very low sensitivity value is achieved close to the open-loop bandwidth of the system, the maximum peak $\|S\|_{\max}$ is only increased a little from 1.85 (5.25 dB) to 1.92 (5.65 dB), which indicates good robustness to the

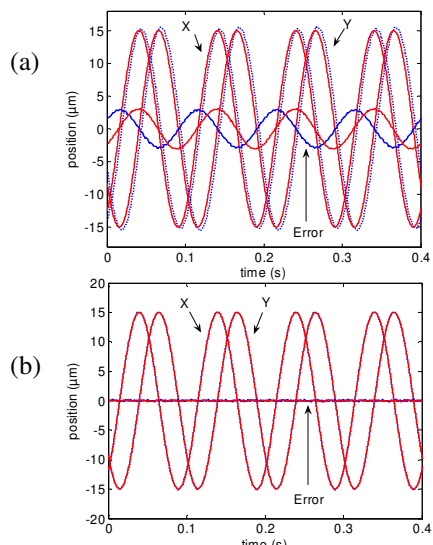


Figure 10. Tracking of 10 Hz sinusoidal waves using normal H_{∞} controller (a) and band focused H_{∞} controller (b).

uncertainties inside the system.

To demonstrate the performance improvement at specific frequency, tracking tests are performed on the stage. In the nano manufacturing or AFM scanning applications, circular motion or sinusoidal inputs with a specific frequency are commonly used. Then controller designed for such a frequency is applied to the system. The results are compared with the normal robust controller in Fig. 10. The command is a circular motion with a 15 μm radius running at 10 Hz. The maximum velocity in X and Y direction is then about 0.95 mm/sec. From Figure 10, it is very clear that the tracking error is compressed greatly. The maximum error decreased from 3 μm with normally designed controller to 150 nm using band focused H_{∞} controller.

VII. CONCLUSION

In this paper, the H_{∞} robust control design is applied for a parallel kinematic nano positioning stage. Due to the parallel kinematic structure, we get a MIMO dynamic system from the actuation to the XYZ motion. The dynamic model of the system is identified experimentally and its order reduced for control design. H_∞ robust control design generates a high bandwidth system and good resolution (<5 nm) for this prototype system. This PKMXYZNP stage is characterized in terms of nonlinearity rejection, resolution and bandwidth, tracking performance. The results demonstrate the advantage of H_{\infty} robust control design as well as parallel kinematic structure for nano positioning. This work demonstrates that high bandwidth systems can be achieved by designing low mass parallel kinematic structures and leaving the burden of handling the resulting complexity due to cross coupling on the control design. The bandwidth of such a system can further be improved by designing stiffer flexure (resulting high natural frequency). Beside normal robust design, a robust control design that gives a significant (over thirty

fold) improvement in tracking of repetitive motions on a prespecified frequency band is also presented which improve the performance greatly even for task frequency close to the bandwidth of the system.

REFERENCES

- [1] H.T.H. Chen, W. Ng, R.L. Engelstad, Finite element analysis of a scanning x-ray microscope micropositioning stage, Review of Scientific Instruments 63 (1) (1992) 591-594.
- [2] K. Sugihara, I. Mori, T. Tojo, C. Ito, M. Tabata, T. Shinozaki, Piezoelectrically driven XYθ table for submicron lithography systems, Review of Scientific Instruments 60 (9) (1989) 3024-3029.
- [3] A. Castaneda, L.M. Apatiga, R. Velazquez, V.M. Castano, Micropositioning device for automatic alignment of substrates for industrial-scale thin films deposition, Assembly Automation 21 (4) (2001) 336-340.
- [4] J.C. Campos Rubio, J.G. Dubuch, A. Vieira Porto, Micropositioning device using solid state actuators for diamond turning machines: a preliminary experiment, Proceedings of SPIE – the International Society for Optical Engineering, 3044 (1997) 317-326.
- [5] S. Stilson, A. McClellan, S. Devasia, High-speed solution switching using piezo-based micropositioning stages, IEEE Transactions on Biomedical Engineering 48 (7) (2001) 806-814.
- [6] A.R. Smith, S. Gwo, C.K. Shih, New high-resolution two-dimensional micropositioning device for scanning probe microscopy applications, Review of Scientific Instruments 65 (10) (1994).
- [7] Y. Li, Q. Xu, A novel design and analysis of a 2-DOF Compliant Parallel Micromanipulator for Nano manipulation, IEEE Transactions on Automation Science and Engineering, 3(3)(2006), 248-253.
- [8] L Lin, M. Tsay, Modeling and control of micropositioning systems using Stewart platforms, Journal of Robotic Systems 17 (1) (2000) 17-52
- [9] B. Yi, H. Na, G.B. Chung, W.K. Kim, I.H. Suh, Design and experiment of a 3DOF parallel micro-mechanism utilizing flexure hinges, Proceedings – IEEE International Conference on Robotics and Automation 2 (2002) 1167-1172.
- [10] Q. Yao, J. Dong, P.M. Ferreira, 2006, "Design, Analysis, Fabrication and Testing of a Piezo-driven Parallel-Kinematics Micropositioning XY Stage", International Journal of Machine Tools & Manufacture, 47, 946–961 (2007).
- [11] S.H. Chen and M. L. Culpepper, Design of a six-axis micro-scale nanopositioner microHexFlex, Precision Engineering, 30(3)(2006), 314-324
- [12] Qing Yao, Jingyan Dong, Placid M. Ferreira, "A Novel Parallel-Kinematics Mechanisms for Integrated, Multi-axis Nano-positioning. Part 1: Kinematics and Design for Fabrications", Precision Engineering, http://dx.doi.org/10.1016/j.precisioneng.2007.03.001.
- [13] J. Dong, Qing Yao, P. M. Ferreira, "A Novel Parallel-Kinematics Mechanisms for Integrated, Multi-axis Nano-positioning. Part 2: Dynamics, Control and Performance Analysis", Precision Engineering, http://dx.doi.org/10.1016/j.precisioneng.2007.03.002.
- [14] Salapaka, S., A. Sebastian, J. P. Cleveland, and M. V. Salapaka. High Bandwidth Nano-Positioner: A Robust Control Approach, Virtual Journal of Nanoscale Science and Technology, 2002.
- [15] A. Sebastian, Salapaka, S., "Design methodologies for robust nanopositioning" IEEE Transactions on control system technology 13(6) (2005) 868-876.
- [16] G. Schitter, P.Menold, H. F. Knapp, F. Allgower, and A. Stemmer, "High performance feedback for fast scanning atomic force microscopes," Review of Scientific Instrument, 72(8), 3320-3327, Aug. 2001.
- [17] Schitter G, Allgower F, Stemmer A. A New Control Strategy or High Speed Atomic Force Microscopy. Nanotechnology 2004, 15(1):108-114.
- [18] Andrew P. Sage and James L. Melsa, System identification, (New York, Academic Press, 1971).
- [19] System identification tool box manual, the MathWorks Inc.